The Astrophysical Journal Letters, 884:L45 (5pp), 2019 October 20 https://doi.org/10.3847/2041-8213/ab4885

Quantifying the Effect of Black Hole Feedback from the Central Galaxy on the Satellite Populations of Groups and Clusters

I. Martín-Navarro[1,2], Joseph N. Burchett[2], and Mar Mezcua[3,4]
[1] Max-Planck Institut für Astronomie, Konigstuhl 17, D-69117 Heidelberg, Germany; imartin@mpia.de
[2] University of California Santa Cruz, 1156 High Street, Santa Cruz, CA 95064, USA
[3] Institute of Space Sciences (ICE, CSCIC), Campus UAB, Carrer de Can Magrans, E-08193, Barcelona, Spain
[4] Institut d'Estudis Espacials de Catalunya (IEEC), C Gran Capità, E-08034 Barcelona, Spain
Received 2019 July 31; revised 2019 September 23; accepted 2019 September 26; published 2019 October 16

Abstract

Supermassive black holes are fundamental ingredients in our theoretical understanding of galaxy formation. They are likely the only sources energetic enough to regulate star formation within massive dark matter halos, but observational evidence of this process remains elusive. The effect of black hole feedback is expected to be a strong function of halo mass, and galaxy groups and clusters are among the most massive structures in the universe. At fixed halo mass, we find an enhanced fraction of quiescent satellite galaxies and a hotter X-ray intragroup and intracluster medium (IGM/ICM) in those groups and clusters hosting more massive black holes in their centers. These results indicate that black hole feedback makes quenching processes more efficient through a cumulative heating of the gaseous IGM and ICM.

Unified Astronomy Thesaurus concepts: Galaxy clusters (584); Intracluster medium (858); Supermassive black holes (1663); Galaxy evolution (594); Galaxy quenching (2040); Star formation (1569)

1. Introduction

In the local universe, every massive dark matter halo, and therefore every massive galaxy, hosts a supermassive black hole in the center (Kormendy & Ho 2013). Supermassive black holes grow in mass mainly through gas accretion (Croton et al. 2006), and the total energy released during this process is on the order of a few percent of the final black hole mass ($M_\bullet$). For black holes more massive than $\sim 10^9$ solar masses ($M_\odot$), the energy released is similar to the binding energy of the host halo itself and can therefore potentially alter the evolution of galaxies residing within. In fact, in state-of-the-art cosmological numerical simulations, the energetic feedback radiated by growing black holes is responsible for reproducing the observed properties of massive galaxies (Schaye et al. 2015; Weinberger et al. 2018). Moreover, the effect of black hole feedback is expected to become increasingly important with increasing halo mass.

Galaxy groups and clusters are massive, gravitationally bound systems, and feedback from the supermassive black hole at the center of the dark matter halo is expected to play a dominant role in regulating their internal thermodynamics. In particular, numerical simulations of galaxy clusters show that the energy injected by the central supermassive black hole into the intragroup/intracluster medium (IGM/ICM) is able to heat the existing gas, preventing the formation of cooling flows (Churazov et al. 2002; Martizzi et al. 2019). Moreover, this feedback is thought to be strong enough to actually regulate the star formation of satellites living within these massive ($M \gtrsim 10^{12}\ M_\odot$) dark matter halos (Dashyan et al. 2019).

Observationally, the clearest indication of the effect of black hole feedback on cluster scales is the existence of large X-ray cavities likely sustained by the energetic input from the central black hole (McNamara & Nulsen 2007; Fabian 2012). However, an empirical assessment of whether black hole feedback actually regulates star formation has proven to be a challenging task. Arguably, the main observational difficulty arises from the fact that black hole feedback is highly nonlinear, with time variations much shorter than those associated with the quenching processes of galaxies (Hickox et al. 2014). The observed connection between the properties of central and satellite galaxies, known as *galaxy conformity* (Weinmann et al. 2006), has also been proposed to be a consequence of the aforementioned black-hole-regulated star formation of the satellite population (e.g., Kauffmann et al. 2013), although it may also arise from the hierarchical nature of a Λ-Cold Dark Matter (Λ-CDM) universe (Bray et al. 2016). Direct observational evidence of black-hole-suppressed star formation therefore stands as a fundamental open question, motivating the development of this study.

In this Letter we explore how the properties of satellite galaxies in groups and clusters depend on the mass of the black hole of the central galaxy. We find that dark matter halos hosting more massive black holes in their centers exhibit an enhanced fraction of quiescent satellites and are able to sustain a hotter IGM/ICM. The outline of this work is as follows. Data are presented in Section 2. We describe our main metric, the $M_\bullet$–$M_{\rm halo}$ relation, in Section 3, and our main results are presented in Section 4. Finally, these results are discussed in Section 5.

2. Data

We have based our analysis on a sample of 4308 galaxy groups and clusters (Tempel et al. 2014) selected from the Sloan Digital Sky Survey (SDSS; Ahn et al. 2014). An extensive discussion about the sample properties is provided in Tempel et al. (2014; see also Section 3.1). We briefly note that group and cluster halo masses and virial radii are measured by assuming that the system is in virial equilibrium. The quoted halo masses and sizes are then estimated using the velocity dispersion and the radial extent of the detected group and cluster members, assuming a Navarro–Frenk–White profile (Navarro et al. 1997). The location of the most luminous galaxy

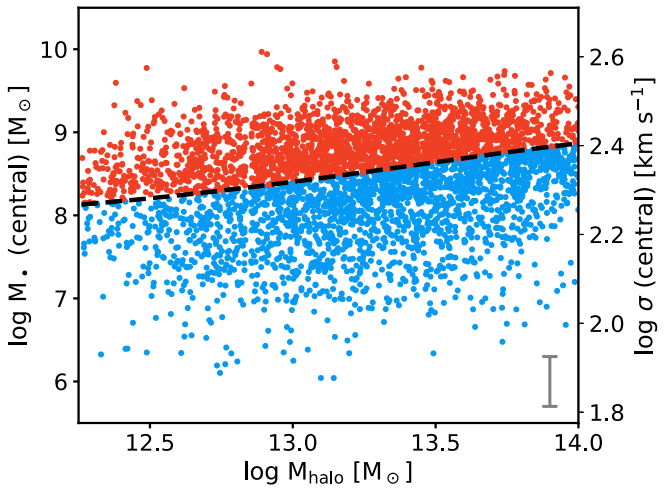

Figure 1. The vertical scatter across the median $M_\bullet$–$M_{\rm halo}$ relation (dashed lined) is a proxy for the total energy released by the central black hole into the IGM/ICM. Overmassive black hole halos (orange dots) have more massive black holes in their centers than undermassive black hole ones (blue dots) and, therefore, should have experienced more intense feedback processes. Each point in this figure corresponds to one of the 4308 SDSS groups and clusters in our sample. Halo masses were calculated through a dynamical modeling of the satellites, while black hole masses were estimated by measuring the stellar velocity dispersion of the central galaxy. The typical uncertainty in the black hole mass estimation is shown in the bottom right corner.

(hereafter central galaxy) is also provided for each object in the catalog. In total, the original catalog contains 82,458 (flux-limited) groups and clusters, at a median redshift of 0.0864, expanding a range in halo mass from $\sim 10^{12}$ to $\sim 10^{14}$ $M_\odot$.

We complemented our sample with total star formation rate (SFR; Brinchmann et al. 2004) and stellar mass (Kauffmann et al. 2003; Salim et al. 2007) measurements also based on the SDSS for each group and cluster member. We did not include in the analysis individual galaxies flagged out by the Max Planck for Astrophysics (MPA) and Johns Hopkins University (JHU) group. Further details on this data set can be found on the MPA–JHU project website.[5]

3. The $M_\bullet$–$M_{\rm halo}$ Relation

In order to explore the connection between central black hole feedback and star formation in satellite galaxies, we first constructed a relation between the group or cluster halo mass ($M_{\rm halo}$) and the mass of the black hole ($M_\bullet$) hosted by the central galaxy as shown in Figure 1. Black hole masses were estimated using the $M_\bullet$–σ_e relation presented in van den Bosch (2016), where stellar velocity dispersions correspond to a fixed aperture of 1 R_e.

For each central galaxy, the velocity dispersion and the redshift were measured from its SDSS optical spectrum using the pPXF algorithm (Cappellari & Emsellem 2004) fed with the MILES stellar population synthesis models (Vazdekis et al. 2010). We then used the measured redshift to estimate the distance to the central galaxy, from which we derived the fraction of its effective radius covered by the SDSS fiber ($R_{\rm SDSS} = 1\farcs5$). Finally, the stellar velocity dispersion at 1 R_e was calculated by applying an aperture correction to the value directly measured from the spectra (Cappellari et al. 2006).

[5] https://wwwmpa.mpa-garching.mpg.de/SDSS/DR7

Having halo and central black hole mass estimations, we calculated the average $M_\bullet$–$M_{\rm halo}$ relation using a two-step running median scheme. First, we measured the median central black hole mass over 150 equally log-spaced halo mass bins (from $\log M_{\rm halo}/M_\odot = 12$ to $\log M_{\rm halo}/M_\odot = 14$). Then, we fit these 150 median halo and central black hole masses with a low-order polynomial. This allowed us to have a well-behaved $M_\bullet(M_{\rm halo})$ function, which is shown in Figure 1 as a black dashed line. The results presented in this Letter are based on a fourth-order polynomial for the $M_\bullet(M_{\rm halo})$ function, but we also repeated the analysis with higher and lower polynomial orders, finding similar and consistent trends.

The $M_\bullet$–$M_{\rm halo}$ relation shown in Figure 1 allowed us to define a metric that is effectively sensitive to the amount of energy radiated by the central black hole (Martín-Navarro et al. 2016; Terrazas et al. 2016). We labeled as *overmassive* black hole halos those systems lying above the mean $M_\bullet$–$M_{\rm halo}$ relation. Complementarily, *undermassive* black hole halos are those that, at a given mass, have a central black hole less massive than the average. The reasoning behind this separation and its relation with the effect of black hole feedback is simple. Halo mass is thought to be the main parameter describing the properties of gravitationally bound structures in a Λ-CDM universe, from individual galaxies to groups and clusters (Blumenthal et al. 1984). Hence the (vertical) scatter in Figure 1 is expected to probe systems with very similar properties but with a variety of central black hole masses. Since the net energy released by supermassive black holes is expected to scale with their total mass from theoretical arguments, feedback-related processes such as galaxy quenching are likely enhanced in overmassive black hole halos compared to undermassive black hole ones. Thus, the scatter in the $M_\bullet$–$M_{\rm halo}$ relation probes the effect of black hole feedback on group and cluster scales, modulo the assumption that overmassive and undermassive black hole halos only differ with respect to their central black hole masses.

3.1. Homogenizing Overmassive and Undermassive Black Hole Halos

It is critical that our approach ensures that there are no systematic differences between overmassive and undermassive black hole halos other than the mass of the central black hole. This is needed to isolate the effect of black hole feedback from possibly confounding variables related to, e.g., cluster assembly (Wechsler & Tinker 2018; Bradshaw et al. 2019). In order to make sure that the overmassive and undermassive black hole halos are as indistinguishable as possible, we adopted the following strategy. For each group and cluster, we identified seven key properties that may potentially affect the measured SFR values: total halo mass, halo size, total stellar mass within the halo, average stellar mass of the lightest and heaviest satellites (10th and 90th percentile by mass, respectively), average stellar mass of those satellites close to the center of the halo (10th percentile in $R/R_{\rm vir}$), and average stellar mass of those satellite galaxies in the outskirts (90th percentile in $R/R_{\rm vir}$). Then, for each overmassive black hole halo we found the most similar undermassive black hole halo in that seven-dimensional parameter space using a Python implementation (Jones et al. 2014) of a KD Tree algorithm (Maneewongvatana & Mount 1999). We finally rejected those systems where no successful match was found (i.e., with a

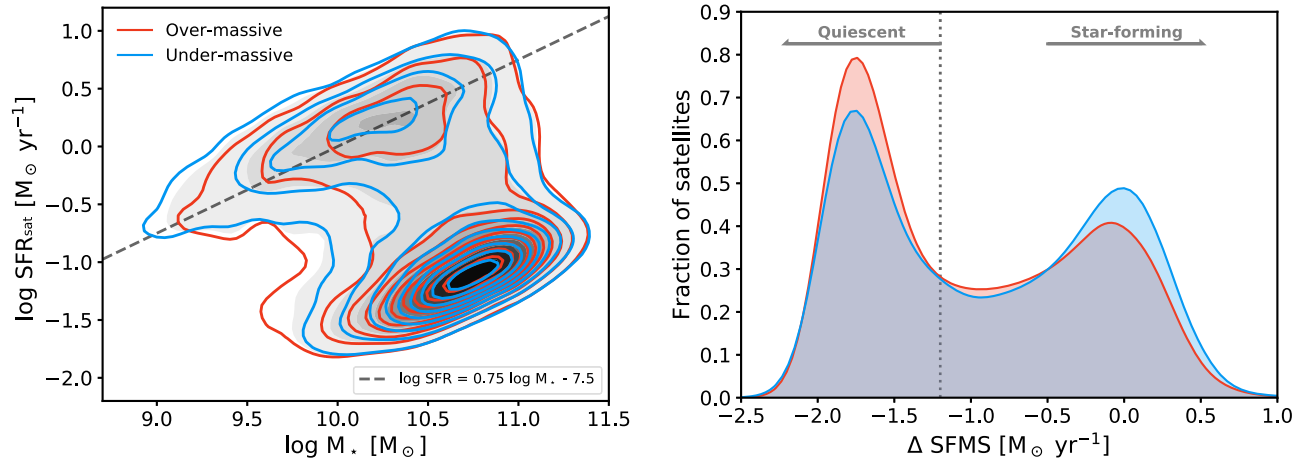

Figure 2. Left: SFR as a function of galaxy stellar mass for satellite galaxies in our sample. Regardless of the mass of the black hole, satellites follow a rather similar star formation main sequence (dashed line). Right: distribution of distances (at fixed mass) with respect to the main sequence (ΔSFMS). The fraction of quiescent satellite galaxies (ΔSFMS < -1.2, vertical dotted line) is different between overmassive (orange) and undermassive (blue) black hole halos, as those groups and clusters with more massive black holes in their center tend to host an enhanced population of quenched satellite galaxies.

normalized KD distance larger than 0.1), leading to a total of 4308 massive halos as indicated above.

3.2. Stellar Velocity Dispersion as a Proxy for M•

The use of stellar velocity dispersion as a proxy for black hole mass has been extensively used in galaxy samples where direct black hole mass measurements are not available (Yu & Tremaine 2002; Marconi et al. 2004; Benson et al. 2007; Bluck et al. 2014). Furthermore, it has been shown that, at fixed stellar mass, varying black hole mass is approximately similar to varying velocity dispersion in relations with stellar population and SFR properties (Martín-Navarro et al. 2019). These findings further support our use of the stellar velocity dispersion as a proxy for black hole mass in our sample.

However, a few important caveats should be noted. First, at fixed stellar velocity dispersion, there are apparent differences in black hole mass (Martín-Navarro et al. 2016), i.e., the intrinsic scatter in the $M_\bullet$–σ relation is not zero (Beifiori et al. 2012). Second, the relation between black hole mass and stellar velocity dispersion might change with galaxy mass, internal structure, and even orientation (Xiao et al. 2011; Graham & Scott 2013; Martín-Navarro & Mezcua 2018; Sahu et al. 2019), which implies that trends with halo mass might be biased (Bernardi et al. 2007). These uncertainties and systematics related to the use of the velocity dispersion as a proxy for black hole mass support our use of a running median to separate overmassive and undermassive black hole halos, which in practice has no other meaning than differentiating the two populations, acknowledging our lack of information about the actual black hole masses.

4. Analysis and Results

Using the $M_{\rm halo}$–$M_\bullet$ relation as a local metric, we then analyzed the SFRs of satellite galaxies in overmassive and undermassive black hole halos. The left panel in Figure 2 shows that non-central members in both overmassive and undermassive black hole halos follow similar distributions in the SFR–stellar mass parameter space, with notably coinciding star formation main sequences (SFMSs) highlighted by the dashed line.[6] However, a striking difference is revealed in the right panel when analyzing the distribution of distances from the main sequence (ΔSFMS): the population of quiescent satellites (ΔSFMS < -1.2)[7] is enhanced in groups and clusters hosting more massive black holes in their centers. Because the number of satellite galaxies in overmassive and undermassive black hole halos is almost identical, by normalization, the number of star-forming galaxies is enhanced in the latter.

In order to investigate the dependence of this effect on halo mass, we binned galaxies in Figure 2 according to the masses of the halos to which they belong. We then calculated the fraction of quiescent satellite galaxies and their average SFR. Figure 3 shows these two quantities for overmassive and undermassive black hole halos as a function of halo mass. The fraction of quiescent galaxies increases and the average SFR decreases with increasing halo mass, as expected (Wetzel et al. 2013). On top of these trends, the differences between overmassive and undermassive black hole halos are clear for all masses. At a given halo mass, when a cluster or a group hosts a more massive black hole in the center, the fraction of quiescent galaxies is enhanced and the average SFR is lower.

A final piece of evidence comes from the analysis of the X-ray properties of 196 optically confirmed groups and clusters (Takey et al. 2013). These systems were identified as extended X-ray sources with an optical galaxy overdensity counterpart detected in the SDSS. Unfortunately, there was little overlap between this sample and that shown in Figure 1, so we did not have a dynamical measurement of the halo mass. Thus, for the analysis of the 196 groups and clusters with X-ray measurements we used M_{500}, an estimate of the average halo mass within an aperture of R_{500} (where the mean mass density is 500 times the critical density of the universe at the halo redshift), rather than $M_{\rm halo}$.[8] This M_{500} halo mass was calculated

[6] The SFMS shown in Figure 2 results from jointly fitting satellite galaxies in overmassive and undermassive black hole halos.

[7] We set this threshold as a conservative limit defining the extension of the red sequence.

[8] For the 22 systems that did overlap between the two samples, we found an approximate conversion of $\log M_{\rm halo} = \log M_{500} - 0.35 \pm 0.11$.

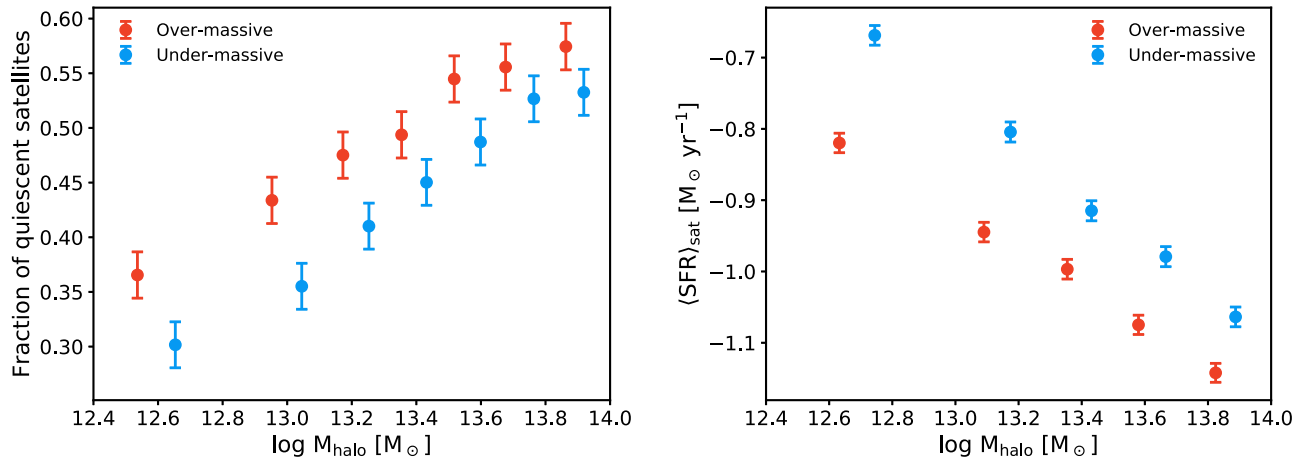

Figure 3. Orange and blue symbols correspond to overmassive and undermassive black hole halos, respectively. Error bars indicate the 1σ uncertainty level. Left: the fraction of quiescent satellite galaxies (ΔSFMS < -1.2) increases with halo mass, but it is always systematically enhanced in groups and clusters with overmassive black holes in their centers. Right: conversely, the median SFR of groups and clusters decreases with increasing halo mass, but it is higher in undermassive black halos because they tend to host fewer quiescent members.

iteratively based on the X-ray bolometric flux assuming a β model (see details in Takey et al. 2011, 2013).

For each of the 196 groups and clusters, the temperature of the IGM/ICM was derived from X-ray spectral fitting (Takey et al. 2011), and the mass of the central black hole was estimated in the same manner as before. As in Figure 1, we divided the sample into overmassive and undermassive black hole halos and then calculated the average X-ray temperature in different mass bins. Figure 4 shows the T_{gas}–M_{500} relation for overmassive and undermassive black hole halos. Two features clearly emerge from this figure. First, as expected by virial arguments (Birnboim & Dekel 2003), X-ray temperatures increase with increasing halo mass (Bogdán et al. 2018). Second, the gas has been heated above the expected virial temperature, and this excess of energy correlates with the mass of the black hole in the center of the halo. At fixed mass, halos with more massive central black holes sustain hotter IGM/ICMs.

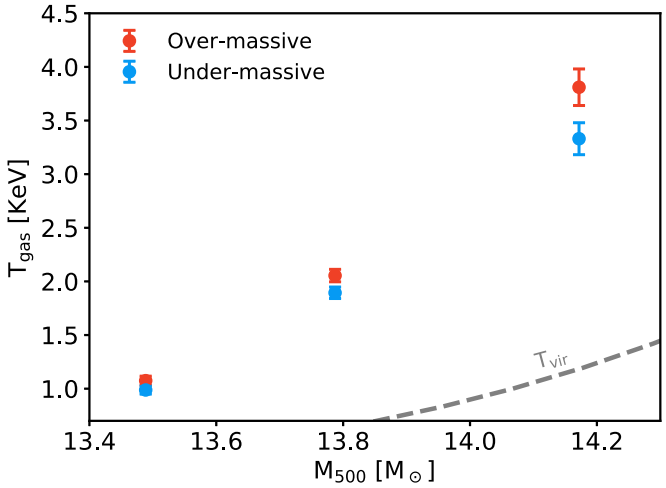

Figure 4. The X-ray gas temperature of the IGM/ICM increases in massive halos for both overmassive (orange symbols) and undermassive (blue symbols) black hole halos, and in all mass bins the temperature is higher than the virial one (dashed line). However, on top of the halo dependence, there is a clear dependence on the mass of the central black hole. At fixed mass, halos with more massive black holes in the center sustain a systematically X-ray hotter IGM/ICM. Error bars indicate the 1σ uncertainty level in the average temperature.

5. Discussion and Conclusion

Explaining the trends shown in Figures 3 and 4 in the absence of feedback from the black hole in the center of the halos would require a highly fine-tuned mechanism. By construction, our overmassive and undermassive black hole halos are indistinguishable in mass, size, total stellar mass, and stellar mass distribution. The effect of a possible assembly bias (Wechsler & Tinker 2018) is likely negligible as there is little difference in the normalization of the SFMS between overmassive and undermassive black hole halos ($\Delta SFMS_0 \sim 0.13 \pm 0.22$). Satellites in groups and clusters with more massive black holes form on average fewer stars, and there is an enhanced fraction of quiescent galaxies compared to undermassive black hole halos, suggesting that longer timescale quenching processes such as strangulation may play a greater role in overmassive black hole halos. A hotter ICM would be more conducive to stripping the gaseous halos of infalling galaxies (Burchett et al. 2018; Zinger et al. 2018), depriving them of their immediate reservoirs for star formation.

Moreover, given the departure from a simple scaling of the virial temperature (dashed line in Figure 4), it is not trivial to explain the higher X-ray temperature of the IGM/ICM in those halos hosting more massive black holes in their centers without invoking feedback effects. Our analysis is certainly a simplified assessment of the effect of black hole feedback. We have assumed that the central galaxy is the only galaxy contributing to the heating of the IGM/ICM. Additionally, group and cluster galaxies likely formed under particular conditions in dense filaments even before falling into the group/cluster environment, and it is therefore possible that some differences between overmassive and undermassive black hole halos have been inherited. We note, however, that SFR measurements are sensitive to timescales much shorter (Calzetti 2013) than the dynamical timescales within halos, and therefore they should be largely driven by recent IGM/ICM conditions.

Black hole heating acting on group and cluster scales emerges as a simple explanation to the observed trends, consistent with our cosmological understanding of galaxy

formation (Dashyan et al. 2019). If the temperatures of halos, and their internal thermodynamics in general, are set by a combination of virial plus black hole heating, quenching processes such as strangulation or ram pressure stripping would become more efficient in those groups and clusters with more massive central black holes, resulting in a higher number of quiescent galaxies as shown in Figure 3. Moreover, this group/cluster-wide feedback process would emerge from accreting black holes in the center of individual massive galaxies, where similar trends between SFR, X-ray temperatures, and black hole masses have been reported (Martín-Navarro et al. 2018, 2019). Interestingly, a unified black hole heating scenario, from galactic to cluster scales, would naturally predict a certain degree of (one halo) galactic conformity (Weinmann et al. 2006; Kauffmann et al. 2013), as quenched galaxies are also found to host higher-mass black holes (Terrazas et al. 2016). Our results observationally support a scenario where the baryonic cycle in galaxies is regulated by the joint effects of black holes and dark matter halos across cosmic time.

We would like to thank the anonymous referee for useful and constructive comments on our manuscript. I.M.N. acknowledges support from the AYA2016-77237-C3-1-P grant from the Spanish Ministry of Economy and Competitiveness (MINECO) and from the Marie Skłodowska-Curie Individual *SPanD* Fellowship 702607. M.M. acknowledges support from the Spanish Juan de la Cierva program (IJCI-2015-23944) and the Beatriu de Pinos fellowship (2017-BP-00114).

ORCID iDs

I. Martín-Navarro https://orcid.org/0000-0003-4266-5580
Joseph N. Burchett https://orcid.org/0000-0002-1979-2197
Mar Mezcua https://orcid.org/0000-0003-4440-259X

References

Ahn, C. P., Alexandroff, R., Allende Prieto, C., et al. 2014, ApJS, 211, 17
Beifiori, A., Courteau, S., Corsini, E. M., & Zhu, Y. 2012, MNRAS, 419, 2497
Benson, A. J., Džanović, D., Frenk, C. S., & Sharples, R. 2007, MNRAS, 379, 841
Bernardi, M., Sheth, R. K., Tundo, E., & Hyde, J. B. 2007, ApJ, 660, 267
Birnboim, Y., & Dekel, A. 2003, MNRAS, 345, 349
Bluck, A. F. L., Mendel, J. T., Ellison, S. L., et al. 2014, MNRAS, 441, 599
Blumenthal, G. R., Faber, S. M., Primack, J. R., & Rees, M. J. 1984, Natur, 311, 517
Bogdán, Á., Lovisari, L., Volonteri, M., & Dubois, Y. 2018, ApJ, 852, 131
Bradshaw, C., Leauthaud, A., Hearin, A., Huang, S., & Behroozi, P. 2019, MNRAS, submitted (arXiv:1905.09353)
Bray, A. D., Pillepich, A., Sales, L. V., et al. 2016, MNRAS, 455, 185
Brinchmann, J., Charlot, S., White, S. D. M., et al. 2004, MNRAS, 351, 1151
Burchett, J. N., Tripp, T. M., Wang, Q. D., et al. 2018, MNRAS, 475, 2067
Calzetti, D. 2013, in Proc. XXIII Canary Islands Winter School of Astrophysics Conf., Secular Evolution of Galaxies, ed. J. Falcón-Barroso & J. H. Knapen (Cambridge: Cambridge Univ. Press), 419
Cappellari, M., Bacon, R., Bureau, M., et al. 2006, MNRAS, 366, 1126
Cappellari, M., & Emsellem, E. 2004, PASP, 116, 138
Churazov, E., Sunyaev, R., Forman, W., & Böhringer, H. 2002, MNRAS, 332, 729
Croton, D. J., Springel, V., White, S. D. M., et al. 2006, MNRAS, 365, 11
Dashyan, G., Choi, E., Somerville, R. S., et al. 2019, MNRAS, 487, 5889
Fabian, A. C. 2012, ARA&A, 50, 455
Graham, A. W., & Scott, N. 2013, ApJ, 764, 151
Hickox, R. C., Mullaney, J. R., Alexander, D. M., et al. 2014, ApJ, 782, 9
Jones, E., Oliphant, T., & Peterson, P. 2014, SciPy: Open Source Scientific Tools for Python, http://www.scipy.org
Kauffmann, G., Heckman, T. M., White, S. D. M., et al. 2003, MNRAS, 341, 33
Kauffmann, G., Li, C., Zhang, W., & Weinmann, S. 2013, MNRAS, 430, 1447
Kormendy, J., & Ho, L. C. 2013, ARA&A, 51, 511
Maneewongvatana, S., & Mount, D. M. 1999, arXiv:cs/9901013
Marconi, A., Risaliti, G., Gilli, R., et al. 2004, MNRAS, 351, 169
Martín-Navarro, I., Brodie, J. P., Romanowsky, A. J., Ruiz-Lara, T., & van de Ven, G. 2018, Natur, 553, 307
Martín-Navarro, I., Brodie, J. P., van den Bosch, R. C. E., Romanowsky, A. J., & Forbes, D. A. 2016, ApJL, 832, L11
Martín-Navarro, I., Burchett, J. N., & Mezcua, M. 2019, MNRAS, submitted
Martín-Navarro, I., & Mezcua, M. 2018, ApJL, 855, L20
Martizzi, D., Quataert, E., Faucher-Giguère, C.-A., & Fielding, D. 2019, MNRAS, 483, 2465
McNamara, B. R., & Nulsen, P. E. J. 2007, ARA&A, 45, 117
Navarro, J. F., Frenk, C. S., & White, S. D. M. 1997, ApJ, 490, 493
Sahu, N., Graham, A. W., & Davis, B. L. 2019, ApJ, 876, 155
Salim, S., Rich, R. M., Charlot, S., et al. 2007, ApJS, 173, 267
Schaye, J., Crain, R. A., Bower, R. G., et al. 2015, MNRAS, 446, 521
Takey, A., Schwope, A., & Lamer, G. 2011, A&A, 534, A120
Takey, A., Schwope, A., & Lamer, G. 2013, A&A, 558, A75
Tempel, E., Tamm, A., Gramann, M., et al. 2014, A&A, 566, A1
Terrazas, B. A., Bell, E. F., Henriques, B. M. B., et al. 2016, ApJL, 830, L12
van den Bosch, R. C. E. 2016, ApJ, 831, 134
Vazdekis, A., Sánchez-Blázquez, P., Falcón-Barroso, J., et al. 2010, MNRAS, 404, 1639
Wechsler, R. H., & Tinker, J. L. 2018, ARA&A, 56, 435
Weinberger, R., Springel, V., Pakmor, R., et al. 2018, MNRAS, 479, 4056
Weinmann, S. M., van den Bosch, F. C., Yang, X., & Mo, H. J. 2006, MNRAS, 366, 2
Wetzel, A. R., Tinker, J. L., Conroy, C., & van den Bosch, F. C. 2013, MNRAS, 432, 336
Xiao, T., Barth, A. J., Greene, J. E., et al. 2011, ApJ, 739, 28
Yu, Q., & Tremaine, S. 2002, MNRAS, 335, 965
Zinger, E., Dekel, A., Kravtsov, A. V., & Nagai, D. 2018, MNRAS, 475, 3654